Synthesis and Characterization of an Organic Soluble and Conducting Polyaniline-Grafted Multiwalled Carbon Nanotube Core–Shell Nanocomposites by Emulsion Polymerization

Jun Xu,[1,2,3] Pei Yao,[1] Litao Liu,[1] Zhongyi Jiang,[2] Fei He,[2] Mei Li,[3] Jingyu Zou[3]

[1]*Center for Analysis, Tianjin University, Tianjin 300072, People's Republic of China*
[2]*School of Chemical Engineering and Technology, Tianjin University, Tianjin 300072, People's Republic of China*
[3]*College of Science, Civil Aviation University of China, Tianjin 300300, People's Republic of China*

Received 23 October 2009; accepted 6 April 2010
DOI 10.1002/app.32581
Published online 29 June 2010 in Wiley InterScience (www.interscience.wiley.com).

ABSTRACT: Organic soluble and conducting polyaniline (PANI)-grafted multiwalled carbon nanotube (MWNT) nanocomposites were synthesized by *in situ* emulsion polymerization. Dodecyl benzene sulfonic acid (DBSA) acted as both a dopant and emulsifier, and phenylamine groups grafted on the surface of the MWNTs via amide bonding joined in the *in situ* polymerization. As self-assembly templates, multiwalled carbon nanotubes containing phenylamine groups (p-MWNTs) were encapsulated by PANI to form a homogeneous core (p-MWNTs)–shell (DBSA-doped PANI) nanostructure. The attachment of soluble DBSA-doped PANI chains on the surface of the p-MWNTs via covalent bonding rendered the p-MWNTs compatible with the polymer matrix and led to the nanocomposite being highly soluble and stable in tetrahydrofuran. The PANI chains grew restrictively on the surface of the p-MWNTs, and the crystalline orders of the PANI coatings were enhanced. Because of the incorporation of the p-MWNTs, the thermal stability of the nanocomposites was improved, and the conductivity of the nanocomposites at room temperature was increased by at least one order of magnitude over neat DBSA-doped PANI. © 2010 Wiley Periodicals, Inc. J Appl Polym Sci 118: 2582–2591, 2010

Key words: conducting polymers; emulsion polymerization; nanocomposites

INTRODUCTION

Among conducting polymers, polyaniline (PANI), because of its good processability, environmental stability, and reversible control of electrical properties by both charge-transfer doping and protonation,[1] is a promising candidate for practical applications in electronic devices. Carbon nanotubes (CNTs), including multiwalled carbon nanotubes (MWNTs) and single-walled carbon nanotubes (SWNTs), with their exceptional structural, mechanical, and electronic properties, have been used in the fabrication of advanced functional materials.[2–5] The combination of PANI with CNTs into composite materials offers opportunities to tailor their properties and introduce new performance on synergetic effects.

For the application of PANI/CNT composites in electronic devices, solubility and processing are key points.[6] To fabricate completely soluble PANI/CNT composites, the improvement of the solubility of PANI and the introduction of strength of binding between PANI and the CNTs to increase the interaction between the components are important aspects. The grafting of soluble PANI and its derivatives on the surface of CNTs is a method for obtaining processable PANI–CNT nanocomposites. Generally, two techniques can be used to obtain CNT graft copolymers. One is the combination of polymer chains with CNTs based on chemical interaction or covalent bonding. The other is the formation or *in situ* polymerization of polymers in the presence of covalently functionalized CNTs. Recent studies have shown that *in situ* polymerization is a good approach for synthesizing homogeneous core (MWNTs)–shell (polymer) nanocomposites that are propitious for exerting synergetic effects from components for electronic and mechanical applications.[7–9] Philip et al.[10] reported that once monomers of PANI are introduced on the surface of MWNTs, they will join in

Correspondence to: P. Yao (pyaotjueducn@163.com).
Contract grant sponsor: Natural Science Foundation of Tianjin People's Republic of China; contract grant number: 08JCYBJC09800.
Contract grant sponsor: National Higher-Education Institutions Research Funding of Civil Aviation University of China; contract grant number: ZXH 2009D008.
Contract grant sponsor: Important Scientific Research Project of Civil Aviation University of China; contract grant number: CAUC2009ZD0202.

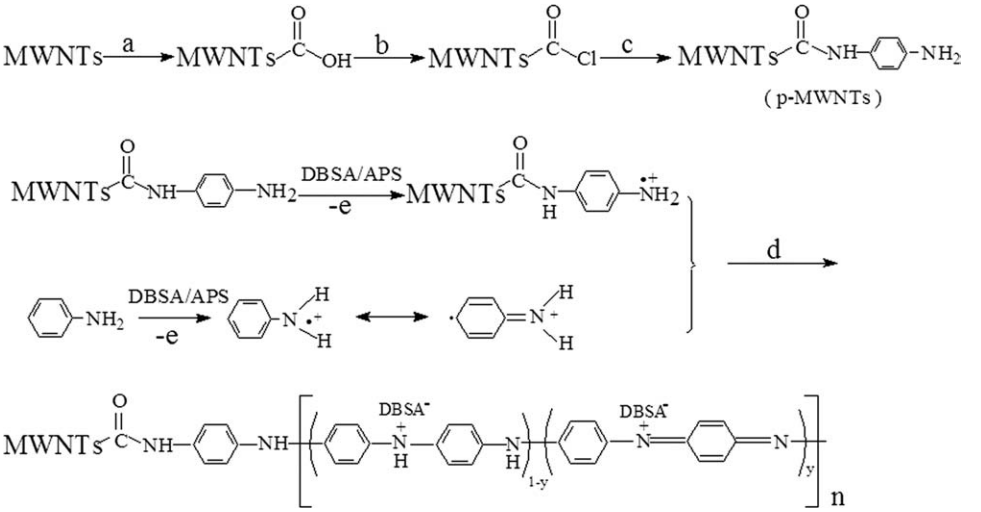

Figure 1 Synthetic process for the DBSA-doped PANI-*g*-MWNT nanocomposites: (a) mixture of concentrated H_2SO_4 and HNO_3 (3 : 1) at 50–60°C ultrasonicated for 12 h, (b) refluxed with $SOCl_2$ in dimethylformamide at 80°C for 24 h, and (c) reacted with p-phenylenediamine at 120°C in dimethylformamide under N_2 for 72 h and (d) *in situ* polymerization of the DBSA-doped PANI-*g*-MWNT nanocomposites.

the polymerization and become a part of the polymer chains, linking between the MWNTs and PANI. This not only helps in the formation of the homogeneous nanostructure but also favors the prevention of potential microscopic phase separation in the composite.

Significant studies have been devoted to the fabrication of soluble or processable PANI and its derivative-grafted CNT nanostructures. For example, Zhao et al.[11] covalently attached poly(aminobenzene sulfonic acid) to SWNTs and obtained a water-soluble graft copolymer. The graft copolymer was a hybrid electronic structure with isolated macromolecular components. Lee et al.[12] functionalized MWNTs with 2,5-diaminobenzene sulfonic acid and further prepared water-soluble and processable poly(diphenylamine sulfonic acid)-grafted MWNTs by *in situ* polymerization. In a previous study,[13,14] we introduced phenylamine groups ($-C_6H_4-NH_2$) the monomers of PANI on the surface of MWNTs [multiwalled carbon nanotubes containing phenylamine groups (p-MWNTs)] and prepared dodecyl benzene sulfonic acid (DBSA)-redoped PANI-grafted MWNT core–shell nanocomposites by *in situ* solution polymerization with dedoping and redoping reactions. Oxidized phenylamine groups grafted on the surface of the p-MWNTs initiated the polymerization, and because of the solubility of PANI and the covalent bonding between the PANI chains and MWNTs, the DBSA-redoped PANI-grafted MWNT nanocomposites were highly soluble and stable in N-methyl-2-pyrrolidinone (NMP).

It is known that the emulsion polymerization method can be used to prepare organic soluble PANI in which functionalized protonic acids, such as dinonylnaphthalenesulfonic acid and DBSA, act as both dopants and emulsifiers.[15,16] PANI–MWNT composites have been synthesized by *in situ* emulsion polymerization.[17,18] Ginic-Markovic et al.[19] reported MWNT–PANI nanocomposites produced by ultrasonically initiated and *in situ* emulsion polymerization. In these composites, the crystallite size and ordered regions of PANI increased, and the thermal stability and electrical conductivity of the composites were higher than those of neat PANI. Because emulsion polymerization is a method for preparing organic soluble PANI, the *in situ* emulsion polymerization of PANI in the presence of covalently functionalized CNTs may become a promising methodology for fabricating PANI-grafted MWNT nanocomposites with solubility and stability in organic solvents, which is significant for the fabrication and application of PANI–CNT composites in electronic devices. However, there are few reports on the preparation and characterization of organic soluble PANI–MWNT nanocomposites by *in situ* emulsion polymerization and CNT grafting technologies.

In this article, we report organic soluble and conducting PANI-grafted MWNT (PANI-*g*-MWNT) nanocomposites prepared by *in situ* emulsion polymerization for the first time to the best of our knowledge. DBSA acted as both a dopant and emulsifier, and phenylamine groups grafted on the surface of the MWNTs (p-MWNTs) joined in the *in situ* polymerization, linking between the polymer chains and MWNTs. As self-assembly templates, the p-MWNTs were encapsulated by PANI to form a homogeneous core–shell nanostructure. The prepared DSBA-doped PANI-*g*-MWNT nanocomposite was completely soluble in tetrahydrofuran (THF) and stable for at least 1 month. The synthetic process for the DBSA-doped PANI-*g*-MWNT nanocomposites is summarized in Figure 1.

EXPERIMENTAL

Reagents and materials

Raw MWNTs (diameter = 20–30 nm, length = 5–15 um) produced by the catalytic chemical vapor deposition (CCVD) method were provided from Chengdu Organic Chemicals Co., Ltd., Chinese Academy of Science R&D Center of Carbon Nanotubes, Chengdu, China. Impurities in the MWNTs may have mixed with functionalized MWNTs, and PANI chains may have grown and accumulated on the irregular particles; this may have impeded the formation of homogeneous nanostructures and decreased the electrical conductivity of the nanocomposites. MWNTs were purified by H_2O_2 oxidation (to remove carbonaceous ones, e.g., amorphous carbon, fullerenes, and nanocrystalline graphite) followed by HCl treatment (to remove metallic catalysts), and the purity of the purified MWNTs was above 95%, as described in ref. 20. p-MWNTs (diameter = 20–30 nm, length = 1.5–5 um) were prepared in our laboratory according to our previous study,[13] in which purified MWNTs were treated with mixture of concentrated acids, refluxed with $SOCl_2$, and then reacted with excess *para*-phenylenediamine. Phenylamine groups ($-C_6H_4-NH_2$) were introduced on the surface of the MWNTs via amide bonding. Hydrochloric acid (36 wt %), nitric acid (65 wt %), and sulfuric acid (98 wt %) were purchased from Tianda Kewei Co., Ltd. (Tianjin, China). Aniline obtained from Jiangtian Chemical Technology Co., Ltd. (Tianjin, China) was distilled and used. DBSA, ammonium peroxydisulfate, acetone, ethanol, and all other organic solvents (analytical grade) were purchased from Tianjin Chemicals Co., Ltd. (Tianjin, China) and were used as received.

Synthesis

The DBSA-doped PANI-*g*-MWNT nanocomposites were synthesized by micellar-aided *in situ* emulsion polymerization. p-MWNTs (93.1 mg) were dispersed in 200 mL of a DBSA aqueous solution (0.04 mol/L) by mechanical stirring and ultrasonication; then, aniline (mass ratio of p-MWNTs to aniline = 1 : 10) was added dropwise to the p-MWNT/DBSA micellar dispersion. After the micellar dispersion was stirred and ultrasonicated for 2 h, 50 mL of an ammonium peroxydisulfate (APS) aqueous solution (0.2 mol/L) was dripped slowly into the reaction system for at least 0.5 h (molar ratio of DBSA to aniline to APS was 0.8 : 1 : 1). The whole synthetic process was controlled at 30°C with constant mechanical stirring and ultrasonication with a KQ-300GDV constant-temperature numerical control ultrasonic wave cleaner working at 40 kHz and 150 W (Kunshan Ultrasonic Instrument Co., Ltd., Jiangsu, China). To investigate the formation mechanism of the nanocomposite, the polymerization was continued for 3 and 6 h. We terminated the reaction by pouring acetone into the black–green emulsion systems; the precipitate cake was filtered and washed with acetone, ethanol, and distilled water to remove unreacted aniline, protonic acid, and oxidant. The products were dried *in vacuo* at 60°C for 12 h. For comparative study, DBSA-doped PANI was prepared under the same conditions without p-MWNTs.

Characterization

Raman spectra of the p-MWNTs and DBSA-doped PANI-*g*-MWNT nanocomposites polymerized for 3 and 6 h were recorded under a Renishaw inVia Raman microscope (Gloucestershire, United Kingdom) with an argon-ion laser operating at 514.5 nm. Fourier transform infrared (FTIR) spectra of the samples in KBr were recorded on a Nicolet Avata 330 spectroscope (Madison, Wisconsin) at room temperature. X-ray photoelectron spectroscopy (XPS) measurements of the DBSA-doped PANI and DBSA-doped PANI-*g*-MWNT composites polymerized for 6 h were carried out with an Electron Spectroscopy for Chemical Analysis (ESCA) PHI-1600 PE XPS spectrometer (Waltham, Massachusetts) with an Mg (Kα) X-ray source. Low-resolution survey scans were performed at 187.85 eV with a step of 0.8 eV, and high-resolution survey scans were performed at 29.35 eV with a step of 0.25 eV. All core-level spectra were referenced to the C1s neutral carbon peak at 284.6 eV and were deconvoluted into Gaussian component peaks. Curve fitting was done by PHI Multipack 8.0 software. The morphology of the nanostructures was determined with an FEI TECNAI G2-F20 field emission transmission electron microscope (Hillsboro, Oregon) operated at 200 kV after the purified MWNTs, p-MWNTs, and DBSA-doped PANI-*g*-MWNT nanocomposites polymerized for 3 and 6 h were dispersed in ethanol and the DBSA-doped PANI-*g*-MWNT composites polymerized for 6 h were dissolved in THF. The crystalline orders of p-MWNTs, DBSA-doped PANI, and DBSA-doped PANI-*g*-MWNT nanocomposites polymerized for 3 and 6 h were carried out by X-ray diffraction (XRD) on a Rigaku D/MAX 2500 V/PC diffractometer (Tokyo, Japan) with Cu/Kα (λ = 1.54056 Å) radiation, and the 2θ scan was in the range 5–50. The thermal stability of the samples and contents of the DBSA-doped PANI coatings on MWNTs were measured with a TA SDTQ600 TG/DTA thermogravimetric analysis (TGA) system (New Castle, DE) at a heating rate of 10°C/min in N_2 from room temperature up to 800°C. The electrical conductivities of the samples were measured by standard four-probe methods with a programmable SDY-5 voltage/current

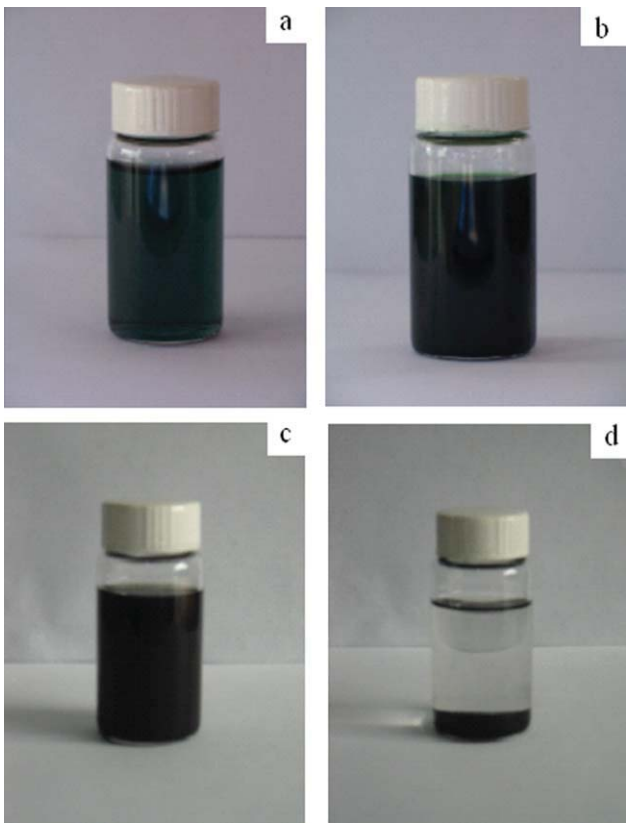

Figure 2 Stability of the (a) DBSA-doped PANI in THF for 1 month, (b) DBSA-doped PANI-*g*-MWNT nanocomposite with a mass ratio of p-MWNTs to aniline of 1 : 10 and polymerized for 6 h in THF for 1 month, (c) p-MWNTs in THF after 1 day, and (d) p-MWNTs in THF after 1 month. [Color figure can be viewed in the online issue, which is available at www.interscience.wiley.com.]

detector (Guangzhou Semi-Conductor Institute, Guangzhou, China) at room temperature. Powder materials of about 100 mg for the p-MWNTs, DBSA-doped PANI, and DBSA-doped PANI-*g*-MWNT nanocomposites polymerized for 3 and 6 h were pressed under 20 MPa into disk pellets 12.7 mm in diameter.

RESULTS AND DISCUSSION

Solubility and stability

The solubility and stability of the DBSA-doped PANI-*g*-MWNT nanocomposites polymerized for 6 h in THF were determined as follows: 1 g of dried powders of the DBSA-doped PANI-*g*-MWNT nanocomposites was added to 30 mL of THF with ultrasonication and stirring for 10 h at room temperature followed by rest for 24 h. The supernatant liquid was carefully transferred into another vessel. The stability of the DBSA-doped PANI, DBSA-doped PANI-*g*-MWNT nanocomposites, and p-MWNTs in THF are shown in Figure 2. The DBSA-doped PANI in THF showed a transparent green solution [Fig. 2(a)], and the DBSA-doped PANI-*g*-MWNT nanocomposites were soluble in THF and formed a black–green solution [Fig. 2(b)]. The nanocomposite was stable in THF, and no floating particles or fallout of small agglomerates appeared in the solution at least for 1 month. After THF in the solution was removed by vacuum drying, the recovered black–green solid matter was weighed. The solubility of the DBSA-doped PANI-*g*-MWNT nanocomposite in THF was measured to be 31.55 mg/mL. After the purified MWNTs were dispersed in THF, fallouts appeared in the suspension, and then, all of the MWNTs settled down at the bottom for 24 h. According to the method mentioned previously, 150 mg of p-MWNTs was dispersed in 20 mL of THF for 10 h at room temperature followed by rest for 24 h. The supernatant liquid showed a black solution, and the solubility of p-MWNTs in THF was measured to be 5.26 mg/mL for 1 day [Fig. 2(c)], which indicated that the stability of p-MWNTs in THF was improved after the phenylamine groups were grafted on the surface of the purified MWNTs via amide bonding. However, the p-MWNTs were not stable in THF as the DBSA-doped PANI-*g*-MWNT nanocomposite. After the solution was rested for 4 more weeks, most of the p-MWNTs settled down at the bottom, as shown in Figure 2(d).

Raman and FTIR analysis

Raman spectra of the p-MWNTs and DBSA-doped PANI-*g*-MWNT nanocomposites polymerized for 3 and 6 h are shown in Figure 3. In the Raman spectrum of the p-MWNTs [Fig. 3(a)], the peak at 1345 cm^{-1} (D mode) indicated the amorphous carbon and disorder, the peak at 1569 cm^{-1} (G mode) revealed the order and integrity of the p-MWNTs, and the shoulder around 1600 cm^{-1} was assigned to the

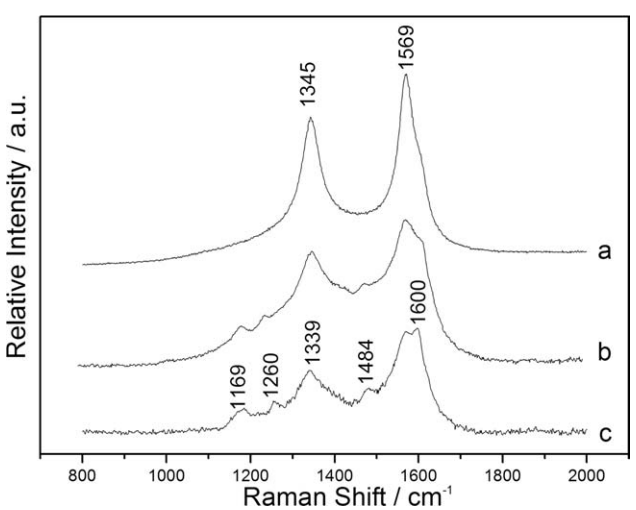

Figure 3 Raman spectra of the (a) p-MWNTs and DBSA-doped PANI-*g*-MWNT nanocomposites with a mass ratio of p-MWNTs to aniline of 1 : 10 and polymerized for (b) 3 and (c) 6 h.

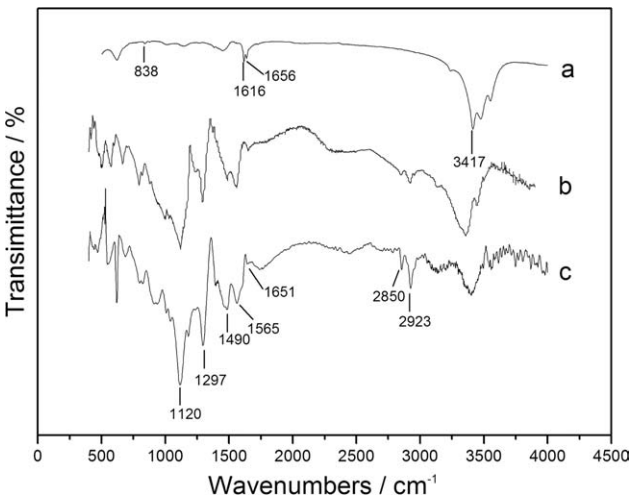

Figure 4 FTIR spectra of the (a) p-MWNTs and DBSA-doped PANI-*g*-MWNT nanocomposites with a mass ratio of p-MWNTs to aniline of 1 : 10 and polymerized for (b) 3 and (c) 6 h.

disorder line.[21,22] The Raman spectrum of the DBSA-doped PANI-*g*-MWNT nanocomposites polymerized for 3 h [Fig. 3(b)] showed doped PANI on the surface of the p-MWNTs. In addition to peaks at 1345 and 1569 cm^{-1} derived from the D mode and G mode of the p-MWNTs, there were C—H bending of the quinoid ring at 1169 cm^{-1}, C—H bending of the benzenoid ring at 1260 cm^{-1}, C=N stretching vibration at 1484 cm^{-1}, C—C stretching of the benzene ring at 1600 cm^{-1}, and C—N^+ stretching at 1339 cm^{-1}. In the Raman spectrum of the nanocomposites polymerized for 6 h [Fig. 3(c)], peaks derived from the p-MWNTs declined, and the typical bands of coated PANI on the MWNTs were enhanced. The phenomena revealed that the p-MWNTs were encapsulated by PANI to form a core (p-MWNTs)–shell (doped PANI) structure in the nanocomposite.[21]

FTIR spectra of the p-MWNTs and DBSA-doped PANI-*g*-MWNT nanocomposites polymerized for 3 and 6 h are shown in Figure 4. In the spectrum of the p-MWNTs [Fig. 4(a)], peaks at 1656 and 1616 cm^{-1} originated from amide I band C=O stretching and amide II band N—H bending; the absorptions at 3417 and 838 cm^{-1} corresponded to amine N—H stretching and the asymmetrical 1,4-disubstituted benzenoid ring, respectively.[10] In the spectra of the DBSA-doped PANI-*g*-MWNT nanocomposites polymerized for 3 and 6 h [Fig. 4(b,c)], the peaks at 1565, 1490, and 1297 cm^{-1} corresponded to C=C stretching of the quinoid rings, C=C stretching of the benzenoid rings, and the C—N stretching mode.[23] The absorptions at 2922, 2850, and 1120 cm^{-1} corresponded to C—H asymmetric stretching vibrations, symmetric stretching vibrations, and the S=O stretching mode of the dopant DBSA.[24,25] Also, there were absorptions at about 1651 cm^{-1} that originated from the carbonyl stretching of the amide bond. These results indicate that the DBSA-doped PANI chains were covalently linked to the p-MWNTs via amide bonding instead of by simple physical wrapping.

XPS analysis

XPS spectra with surface elements and quantitative analysis for the DBSA-doped PANI and DBSA-doped PANI-*g*-MWNT nanocomposites polymerized for 6 h and the deconvolution of the N1s spectrum of the nanocomposite are shown in Figure 5. In the spectra of both samples, not only elements present, but also atomic concentrations on the surface of the nanocomposite were closed to those of the neat DBSA-doped PANI. The result indicates that in the composite, the p-MWNTs were wrapped underneath the PANI coatings to form a core (p-MWNTs)–shell (DBSA-doped PANI) nanostructure, which was consistent with the Raman analysis mentioned previously. As shown in Figure 5(c), N1s of the DBSA-doped PANI-*g*-MWNT nanocomposites could be deconvoluted to three peaks[26,27] centered at 399.39 eV (originating from —NH—), 400.73 eV (originating from $=N^+-$), and 402.03 eV (originating from $-N^+-$) with area fractions of 48.84, 23.15, and 28.12%, respectively. The N^+/N ratio of the PANI coatings was 51.15%. The results illuminate $CH_3(CH_2)_{11}C_6H_4SO_3^-$ as counter ions located around positively charged nitrogen, and the PANI coatings were highly doped by DBSA in Emeraldine Salt form.

Morphology

TEM images of the purified MWNTs, p-MWNTs, DBSA-doped PANI-*g*-MWNT nanocomposites polymerized for 3 and 6 h dispersed in ethanol, and nanocomposite polymerized for 6 h dissolved in THF are shown in Figure 6. Figure 6(a1,a2) shows the integrate and smooth sidewalls of the purified MWNTs; there were few defects, and amorphous layers presented on the surface. Figure 6(b1,b2) shows the rough sidewalls of the p-MWNTs and functional groups, such as phenylamine groups on the surface of the p-MWNTs. In the images of the nanocomposites polymerized for 3 h [Fig. 6(c1,c2)], there were prominences lying along the sidewall of the p-MWNTs and heaps located at the ends of the p-MWNTs. In the images of the nanocomposites polymerized for 6 h [Fig. 6(d1,d2)], the p-MWNTs were encapsulated by homogeneous and uniform PANI coatings, and the diameters of the nanostructures were in the range 110–120 nm.

The morphology of the nanocomposites revealed the nature of PANI chain growth on the surface of

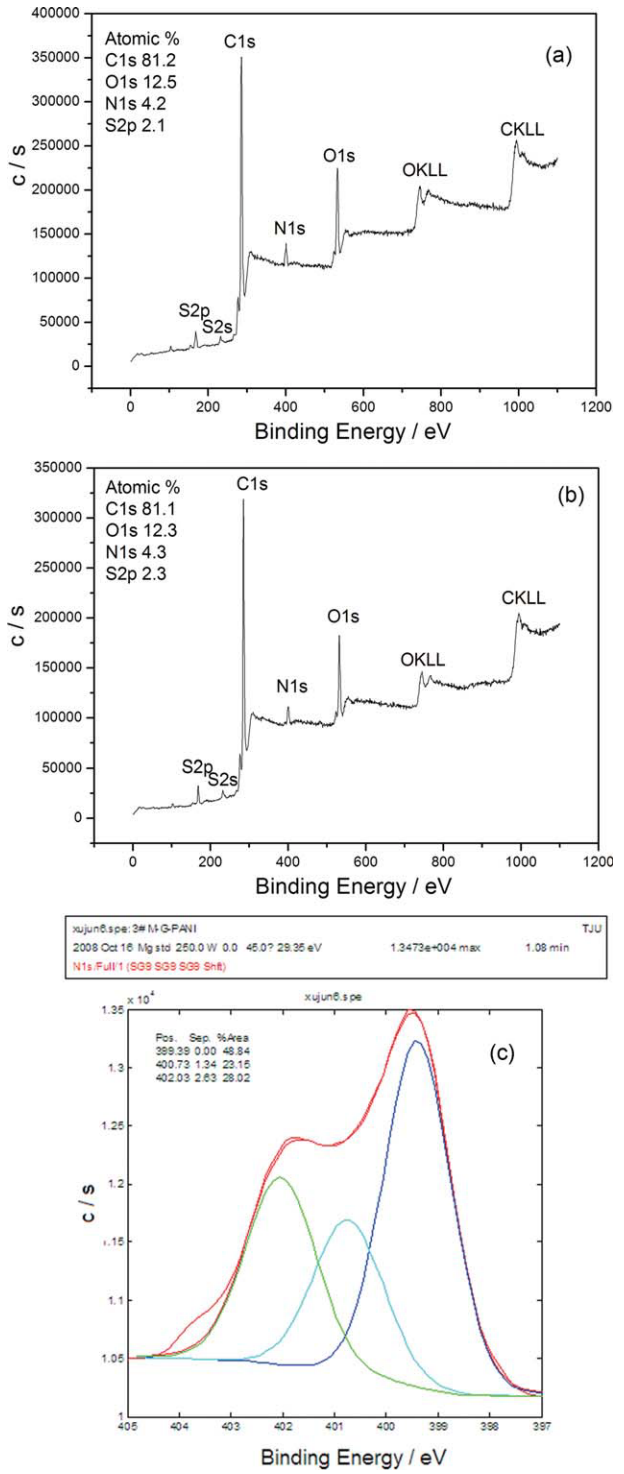

Figure 5 Wide-scan XPS spectra of the (a) DBSA-doped PANI, (b) DBSA-doped PANI-*g*-MWNT nanocomposite with a mass ratio of p-MWNTs to aniline of 1 : 10 and polymerized for 6 h, and (c) deconvolution of N1s for the nanocomposite. [Color figure can be viewed in the online issue, which is available at www.interscience.wiley.com.]

the p-MWNTs. After the p-MWNTs were dispersed in DBSA aqueous solution, the p-MWNTs were surrounded by emulsifier, and p-MWNT/DBSA micellars were formed. As aniline monomers were added, some monomers entered into the p-MWNT/DBSA micellars and absorbed on the surface of the p-MWNTs; other monomers were surrounded by emulsifier and formed monomer droplets. Because the surface area of the p-MWNT/DBSA micellars was far larger than that of the monomer droplets, most of the radicals produced by APS decomposition were caught by the p-MWNT/DBSA micellars. In the p-MWNT/DBSA micellars, oxidized phenylamine groups on the surface of the p-MWNTs initiated polymerization, which dominated the formation of an inner layer of PANI coatings and PANI heaps at tube ends. Although oxidized aniline cation radicals noncovalently linked with the p-MWNTs formed the polymer chains far from the surface of the p-MWNTs and were mainly distributed in the outer layer of PANI coatings,[10] to decrease surface energy and interfacial tension, PANI chains in the outer layers preferentially accumulated in the valleys between prominences along the surface of the p-MWNTs, which increased the average diameter of the core–shell nanostructures and helped to form uniform PANI coatings.[13]

When the nanocomposites polymerized for 6 h dissolved in THF [Fig. 6(e1,e2)], a part of the PANI coatings were dissolved in solvent, the core–shell structures were not changed, and there was swelling along the PANI coatings. The morphology naturally accounted for the high stability of the nanocomposite dissolved in THF. There were two kinds of soluble PANI chains assembled on the surface of the p-MWNTs. One was covalently attached to the p-MWNTs via amide bonding; the other was noncovalently linked with the p-MWNTs.[10,13,14] When the nanocomposite was dispersed in THF, most of the latter (PANI chains none covalently linked with p-MWNTs) was dissolved in THF, as shown in the thin films and dissociative small pieces far away from the MWNTs in Figure 6(e1), whereas the polymer chains covalently attached to the p-MWNTs swelled along the surface of the p-MWNTs [Fig. 6(e2)]. As a result, the nanocomposite was stabilized in THF via the strengthening of chemical bonding between the CNTs and PANI and the solubility of the polymer chains.

XRD analysis

XRD patterns for the p-MWNTs, DBSA-doped PANI, and DBSA-doped PANI-*g*-MWNT nanocomposites with different reaction times are presented in Figure 7. In the XRD diffractogram of the p-MWNTs [Fig. 7(a)], the intense peak around $2\theta = 25.9^\circ$ and low peaks around 43–44° were derived from the graphitelike structure and catalytic particles inside the walls of the CNTs.[28] In the XRD pattern of the DBSA-doped PANI [Fig. 7(b)], the peaks at $2\theta = 19.8$

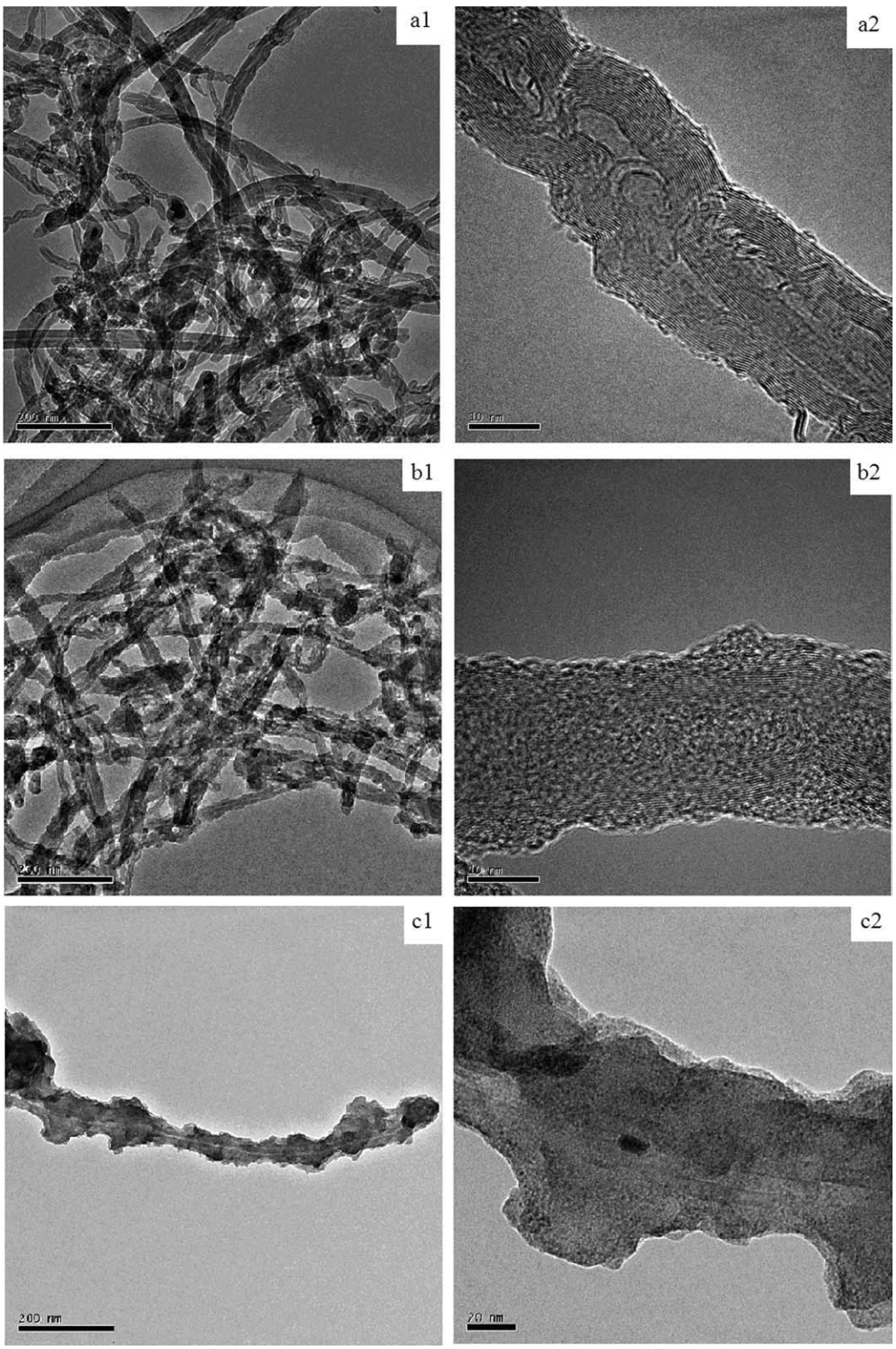

Figure 6 TEM images of the (a) purified MWNTs [(a1) scale bar = 200 nm, (a2) scale bar = 10 nm] in ethanol, (b) p-MWNTs [(b1) scale bar = 200 nm, (b2) scale bar = 10 nm] in ethanol, DBSA-doped PANI-*g*-MWNT nanocomposites with a mass ratio of p-MWNTs to aniline of 1 : 10 and polymerized for (c) 3 h [(c1) scale bar = 200 nm, (c2) scale bar = 20 nm] and (d) 6 h [(d1) scale bar = 200 nm, (d2) scale bar = 20 nm] in ethanol, and (e) DBSA-doped PANI-*g*-MWNT nanocomposite polymerized for 6 h and dissolved in THF [(e1) scale bar = 200 nm, (e2) scale bar = 20 nm].

and 25.2° arose from the (020) and (200) reflections, respectively, of PANI in its ES form.[29] Compared with that of neat PANI, the XRD diffractograms of the DBSA-doped PANI-*g*-MWNT nanocomposites [Fig. 7(c,d)] presented crystalline peaks at 9.6, 15.5, and 29.6° assigned to the (001), (011) and (022)

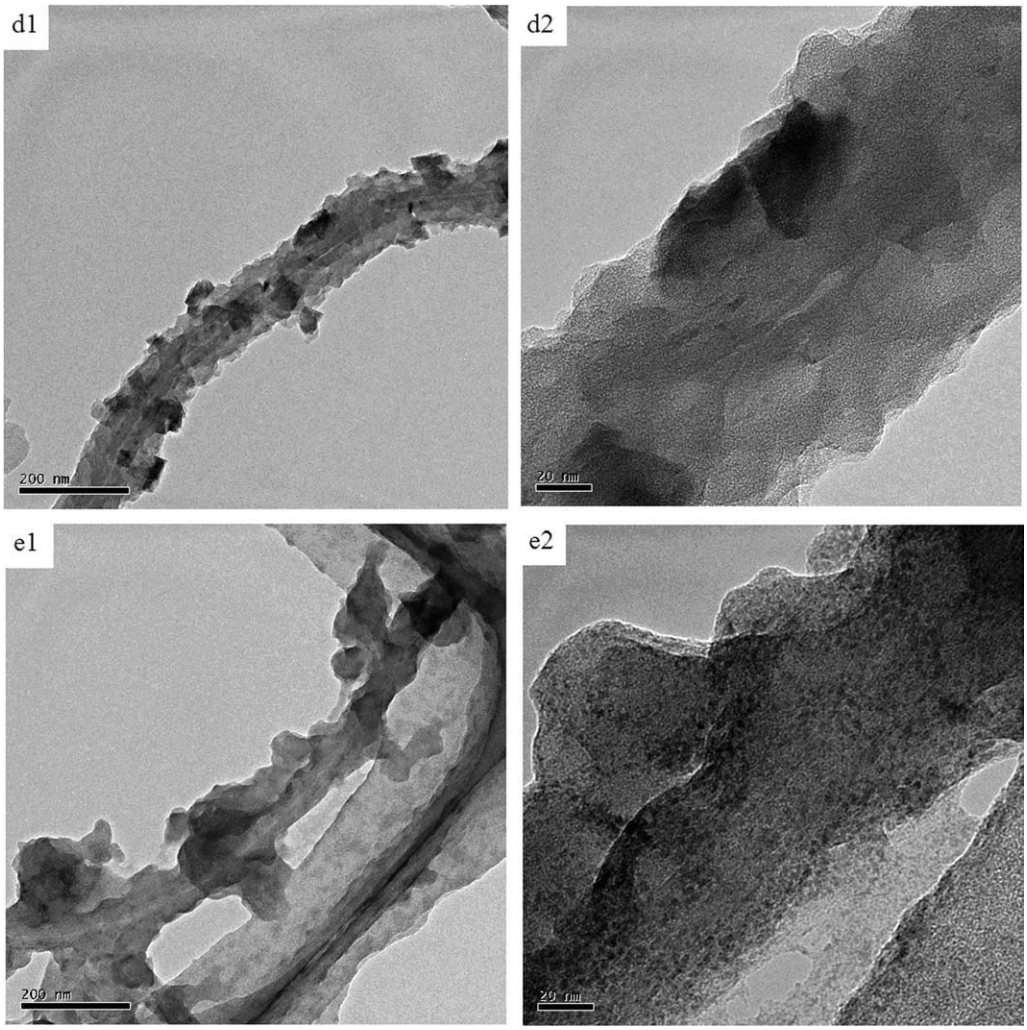

Figure 6 (Continued from the previous page)

reflections, respectively, of Polyaniline Emeraldine Salt.[29,30] All diffraction peaks of the nanocomposites polymerized for 3 h were more detectable. These indicated that within an earlier reaction period, the polymer chains were highly ordered, and microcrystalline domains were enriched in the PANI inner layers. With increasing reaction time, PANI chains deposited under less restrictive conditions, and more amorphous parts were distributed in the field far from the surface of the p-MWNTs. As a whole, the order of the polymer chains in the PANI coatings increased compared with neat DBSA-doped PANI.

TGA

The TGA curves of the p-MWNTs, DBSA-doped PANI-*g*-MWNT nanocomposites polymerized for 3 and 6 h, and DBSA-doped PANI are shown in Figure 8. The weight loss of all of the samples below 200°C was attributed to the release of moisture and low-molecular-weight oligomers along surface of the samples. The p-MWNTs [Fig. 8(a)] displayed a weight loss of 7.68% in the interval of 200–400°C because of the decomposition of phenylamine groups grafted on the surface of the p-MWNTs; after that, the p-MWNTs showed a steady weight loss for further decomposition.[13] DBSA-doped PANI [Fig. 8(d)] showed a weight loss of 37.46% in the interval of 200–340°C from the dedoping process and then the burning of PANI and leftovers in the range 330–800°C. The TGA curves of the DBSA-doped PANI-*g*-MWNT nanocomposites polymerized for 3 and 6 h [Fig. 8(b,c)] comprised a dedoping process at 200–320°C, a platform with mild decomposition speed in the range 310–410°C, and then the burning of PANI and leftovers in the range 410–800°C. The different thermal behaviors illuminated the presence of MWNTs in PANI and the existence of a new phase in the nanostructures.[31] The weight loss behaviors after the dedoping process of PANI in the nanocomposites were controlled by both the degradation of the polymer chains and the decomposition of covalent bindings between PANI and MWNTs in the new phase.[13] According to the

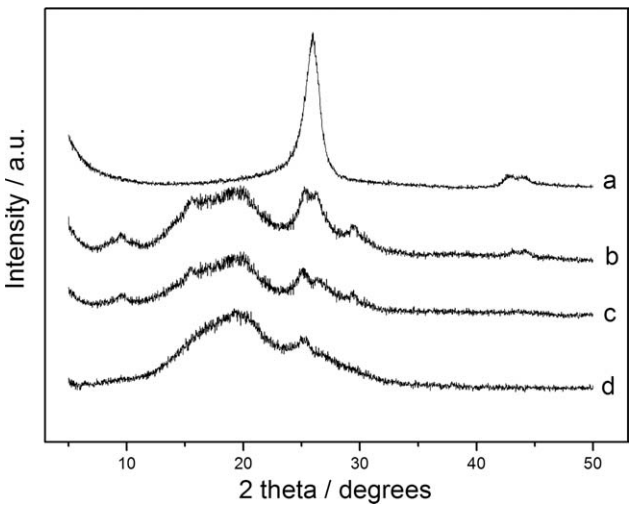

Figure 7 XRD diffractogram of the (a) p-MWNTs and DBSA-doped PANI-*g*-MWNT nanocomposites with a mass ratio of p-MWNTs to aniline of 1 : 10 and polymerized for (b) 3 and (c) 6 h and (d) DBSA-doped PANI.

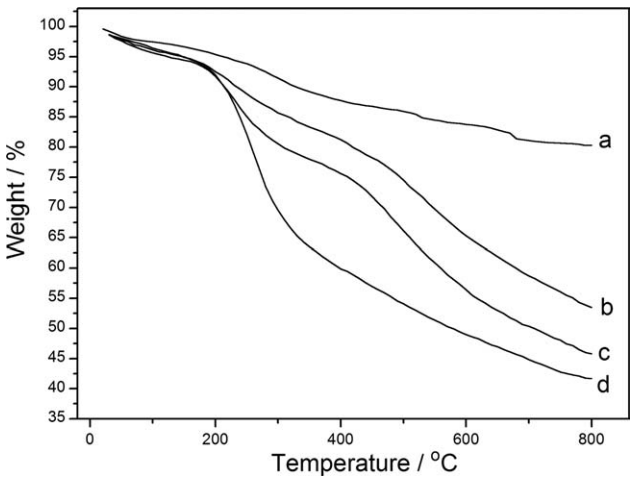

Figure 8 TGA curves of the (a) p-MWNTs and DBSA-doped PANI-*g*-MWNT nanocomposites with a mass ratio of p-MWNTs to aniline of 1 : 10 and polymerized for (b) 3 and (c) 6 h and (d) DBSA-doped PANI.

weight losses of the p-MWNTs, DBSA-doped PANI-*g*-MWNT nanocomposites, and DBSA-doped PANI from 200 to 800°C, the contents of the PANI coatings on the p-MWNTs in the nanocomposites polymerized for 3 and 6 h were estimated to be 82.75 and 94.86%, respectively.

Conductivity

The electrical conductivities at room temperature for the p-MWNTs, DBSA-doped PANI, and DBSA-doped PANI-*g*-MWNT nanocomposites polymerized for 3 and 6 h were 71.69, 1.03×10^{-2}, 13.65, and 6.23×10^{-1} S/cm, respectively. Within the earlier reaction period, the polymer chains grew restrictively on the surface of the p-MWNTs, and microcrystalline domains were enriched in the PANI inner layers. The ordered structures and high weight percentages of p-MWNTs led to a conductivity increase to 13.65 S/cm in the DBSA-doped PANI-*g*-MWNT nanocomposite polymerized for 3 h. With increasing reaction time, the weight percentage of p-MWNTs decreased, and more amorphous parts were distributed in the outer layers of the PANI coatings. Also, the ultrasonic process is a method for producing MWNTs in short tubes.[32] The p-MWNTs were cut by continuous ultrasonication in the polymerization. Low-resolution TEM images of the nanocomposites are shown in Figure 9. As shown in Figure 9(a),

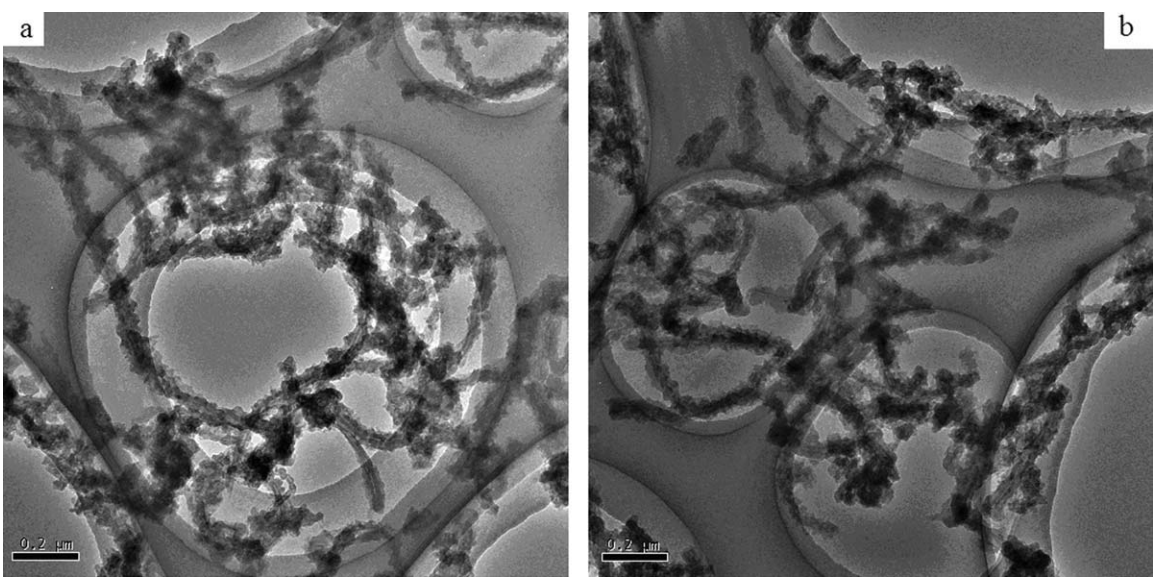

Figure 9 TEM images of DBSA-doped PANI-*g*-MWNT nanocomposites with a mass ratio of p-MWNTs to aniline of 1 : 10 and polymerized for (a) 3 h (scale bar = 0.2 μm) and (b) 6 h (scale bar = 0.2 μm).

most of the nanostructures polymerized for 3 h were 1–3 μm in length with diameters of about 100 nm (aspect ratio = 10–30). As shown in Figure 9(b), most of the nanostructures polymerized for 6 h were 0.3–1.5 μm in length with diameters of about 120 nm (aspect ratio = 2.5–12.5). Compared with the sample polymerized for 3 h, there were more shortened core–shell nanostructures in the sample polymerized for 6 h. Continuous ultrasonication decreased the integrity of the p-MWNTs and cut p-MWNTs, and shortened core–shell nanostructures affected the charge transport in the nanocomposite. As a result of these aspects, the conductivity of the nanocomposites polymerized for 6 h decreased to 6.23×10^{-1} S/cm. On the other hand, the p-MWNTs increased the effective charge delocalization and provided efficient matrix for charge transport in the PANI conducting domains; carrier transportation may have been restricted to the boundary or interface between the MWNTs and PANI inner layers,[30] in which phenylamine groups grafted on the surface of the p-MWNTs acted as bridges to facilitate charge delocalization. As a whole, the electrical conductivity at room temperature of the DBSA-doped PANI-*g*-MWNT nanocomposites increased by at least one order of magnitude over neat DBSA-doped PANI.

CONCLUSIONS

DBSA-doped PANI-*g*-MWNT conducting nanocomposites with solubility and stability in organic solutions were synthesized by *in situ* emulsion polymerization. Phenylamine groups grafted on the surface of the p-MWNTs joined in the *in situ* polymerization and acted as chemical bridges between the p-MWNTs and soluble PANI chains. As self-assembly templates, p-MWNTs are encapsulated by DBSA-doped PANI to form a homogeneous core–shell nanostructure. Attachment of soluble DBSA-doped PANI chains on the surface of the p-MWNTs via covalent bonding rendered the p-MWNTs compatible with the polymer matrix and led to the DBSA-doped PANI-*g*-MWNT nanocomposites achieving stability for at least 1 month and a solubility of 31.55 mg/mL in THF. The PANI chains grew restrictively on the surface of the p-MWNTs, and the order of polymer chains in the PANI coatings increased. Because of the incorporation of the p-MWNTs, the thermal stability of the nanocomposites was improved after the dedoping process of the PANI coatings, and the conductivity of the nanocomposite at room temperature was increased by at least one order of magnitude over neat DBSA-doped PANI.

References

1. Ghosh, P.; Siddhanta, S. K.; Chakrabarti, A. Eur Polym J 1999, 35, 699.
2. Iijima, S.; Ichihashi, T. Nature 1993, 363, 603.
3. Iijima, S. Nature 1991, 354, 56.
4. Ajayan, P. M.; Stephan, O.; Colliex, C.; Trauth, D. Science 1994, 265, 1212.
5. Wong, E. W.; Sheehan, P. E.; Lieber, C. M. Science 1997, 277, 1971.
6. Sainz, R.; Benito, A. M.; Martinez, M. T.; Galindo, J. F.; Sotres, J.; Baŕo, A. M.; Corraze, B.; Chauvet, O.; Dalton, A. B.; Baughman, R. H.; Maser, W. K. Nanotechnology 2005, 16, S150.
7. Zhang, X.; Zhang, J.; Liu, Z. Appl Phys A 2005, 80, 1813.
8. Wu, T.-M.; Lin, Y.-W. Polymer 2006, 47, 3576.
9. Gopalan, A. I.; Lee, K.-P.; Santhosh, P.; Kim, K. S.; Nho, Y. C. Compos Sci Technol 2007, 67, 900.
10. Philip, B.; Xie, J.; Abraham, F. J. K.; Varadan, V. K. Polym Bull 2005, 53, 127.
11. Zhao, B.; Hu, H.; Yu, A.; Perea, D.; Haddon, R. C. J Am Chem Soc 2005, 127, 8197.
12. Lee, K. P.; Gopalan, A. Y.; Kim, K. S.; Santhosh, P. J Nanosci Nanotech 2007, 7, 3386.
13. Xu, J.; Yao, P.; Li, X.; He, F. Mater Sci Eng B 2008, 151, 210.
14. Yao, P.; Xu, J.; Wang, Y.; Zhu, C. J Mater Sci Mater Electron 2009, 20, 891.
15. Kinlen, P. J.; Liu, J.; Ding, Y.; Graham, C. R.; Remsen, E. E. Macromolecules 1998, 31, 1735.
16. Kim, J.; Kwon, S.; Ihm, D. W. Curr Appl Phys 2007, 7, 205.
17. Jeevananda, T.; Siddaramaiah; Lee, T. S.; Lee, J. H.; Samir, O. M.; Somashekar, R. J Appl Polym Sci 2008, 109, 200.
18. Zelikman, E.; Narkis, M.; Siegmann, A.; Valentini, L.; Kenny J. M. Polym Eng Sci 2008, 48, 1872.
19. Ginic-Markovic, M.; Matisons, J. G.; Cervini, R.; Simon, G. P.; Fredericks, P. M. Chem Mater 2006, 18, 6258.
20. Feng, Y.; Zhou, G.; Wang, G. P. Chem Phys Lett 2003, 375, 645.
21. Wu, T.-M.; Lin, Y.-W. Polymer 2006, 47, 3576.
22. Rao, A. M.; Jorio, A.; Pimenta, M. A.; Dantas, M. S. S.; Saito, R.; Dresselhaus, G.; Dresselhaus, M. S. Phys Rev Lett 2000, 84, 1820.
23. Yu, Y.; Che, B.; Si, Z.; Li, L.; Chen, W.; Xue, G. Synth Met 2005, 150, 271.
24. Chang, K.-C.; Jang, G.-W.; Peng, C.-W.; Lin, C.-Y.; Shieh, J.-C.; Yeh, J.-M.; Yang, J.-C.; Li, W.-T. Electrochim Acta 2007, 52, 5191.
25. Lei, X.; Liu, Y.; Su, Z. Polym Compos 2008, 29, 239.
26. Li, Z. F.; Kang, E. T.; Neoh, K. G.; Tan, K. L. Synth Met 1997, 87, 45.
27. Li, Z. F.; Neoh, K. G.; Pun, M. Y.; Kand, E. T.; Tan, K. L. Synth Met 1995, 73, 209.
28. Chaudhari, H. K.; Kelkar, D. S. Polym Int 1997, 42, 380.
29. Gupta, M. C.; Umare, S. S. Macromolecules 1992, 25, 138.
30. Feng, W.; Bai, X. D.; Lian, Y. Q.; Liang, J.; Wang, X. G.; Yoshino, K. Carbon 2003, 41, 1551.
31. Sainz, R.; Benito, A. M.; Martínez, M. T.; Galindo, J. F.; Sotres, J.; Baró, A. M.; Corraze, B.; Chauvet, O.; Maser, W. K. Adv Mater 2005, 17, 278.
32. Park, H. J.; Park, M.; Chang, J. Y.; Lee, H. Nanotechnology 2008, 19, 335702.